Soil movements on permafrost slopes near Fairbanks, Alaska

TIEN H. WU

The Ohio State University, 2070 Neil Avenue, Columbus, OH 43210, U.S.A.

Received January 9, 1984

Accepted July 13, 1984

Many north-facing slopes in the Yukon–Tanana Uplands of Alaska show signs of downhill movements in the form of hummocky surface and leaning trees. Measurements of movements and pore pressures were made at several sites in the Caribou–Poker Creek Research Watershed. It was found that, on slopes with inclinations near 30°, most of the movements occurred immediately after thaw when pore pressures were high.

To evaluate the slope stability, the soil strength was measured by direct shear tests. The strength of the moss layer and tree roots was evaluated by performing tension tests on the roots and the moss–root complex. Results of stability analyses show that local failures involving individual wedges are likely. The displacements associated with a wedge slide would result in a hummock or step. The strength of the moss–root complex was found to be a significant factor in the stability of the wedge and of the step.

Key words: moss, roots, permafrost, pore pressure, shear strength, slope stability, thaw.

De nombreuses pentes orientées vers le nord dans les Yukon–Tanana Uplands en Alaska montrent des signes de mouvement sous la forme de surface ondulée et d'arbres inclinés. Des mesures de déplacement et de pressions interstitielles ont été faites sur plusieurs sites dans le bassin versant expérimental du ruisseau Caribou–Poker. On a constaté que, pour les pentes ayant une inclinaison proche de 30°, la plupart des mouvements se produisent immédiatement après le dégel, lorsque les pressions interstitielles sont fortes.

Pour évaluer la stabilité des pentes, la résistance au cisaillement du sol a été mesurée par essai de cisaillement direct. La résistance au cisaillement de la couche de mousse et des racines d'arbre a été évaluée à partir d'essais de traction sur le complexe racine–mousse. Les résultats des analyses de stabilité montrent que des ruptures locales impliquant des blocs individuels sont probables. Les déplacements associés à un glissement de bloc devraient résulter en une surface ondulée ou en escaliers. La résistance du complexe racine–mousse s'est avérée être un facteur important dans la stabilité d'un bloc et d'un décrochement.

Mots clés: mousse, racines, pergélisol, pression interstitielle, résistance au cisaillement, stabilité des pentes, dégel.

[Traduit par la revue]

Can. Geotech. J. **21**, 699–709 (1984)

Introduction

The Yukon–Tanana Uplands of Alaska (Wahrhaftig 1965) is located in the zone of discontinuous permafrost. The north-facing slopes are usually underlain by permafrost and support a forest composed mostly of black spruce (*Picea mariana*) with small numbers of paper birch (*Betula papyrifera*). Trees that lean downhill are common on the steeper north-facing slopes. The surface of these slopes is, in many places, uneven and hummocky. Other than the vegetation, the hummocks resemble very closely the "steps" described by Washburn (1980). For this reason, the term step is used here, although the mechanism responsible for their formation may well be different from those described by Washburn. This paper describes an investigation of the stability of several of these slopes. The objectives were to determine whether movements occur on these slopes and if so, to establish the mechanics of the movements.

Site conditions

The area chosen for study is located in the Caribou–Poker Creek Research Watershed near Fairbanks, AK (Slaughter 1971). From reconnaissance of the valleys of Caribou and Little Poker Creeks, steps and benches that suggest movements were found to be limited to relatively steep north-facing slopes of about 30° or more. These slopes are poorly drained and are covered with a sparse growth of black spruce. The vegetation is classified as evergreen low savana: black spruce/sphagnum (Viereck 1975). Some of these areas are indicated as D, E, F, G in the air photograph (Fig. 1).

Five sections, A, B, D, E, F, located along Caribou Creek (Fig. 1), were chosen for study. A and B represent comparatively flat slopes with no visible signs of movement. D, E, and F show progressively more serious signs of movement such as leaning and bent trees (Fig. 2) and steps (Washburn 1980) that measure about 3 × 3 m in area. Just west of profile F is an old slide scar.

The soils at the site belong to the Ester series according to Rieger *et al.* (1972). A layer of brown silt of variable thickness lies underneath the moss. The silt is believed to be windblown in origin, but contains rock fragments derived from the bedrock. The percentage of rock fragments generally increases with depth. Excavations were stopped when it became impossible to dislodge the rock fragments. Hence the bottom of the auger hole is taken as the bottom of the soil profile. At some locations, a gray silt, which was probably derived

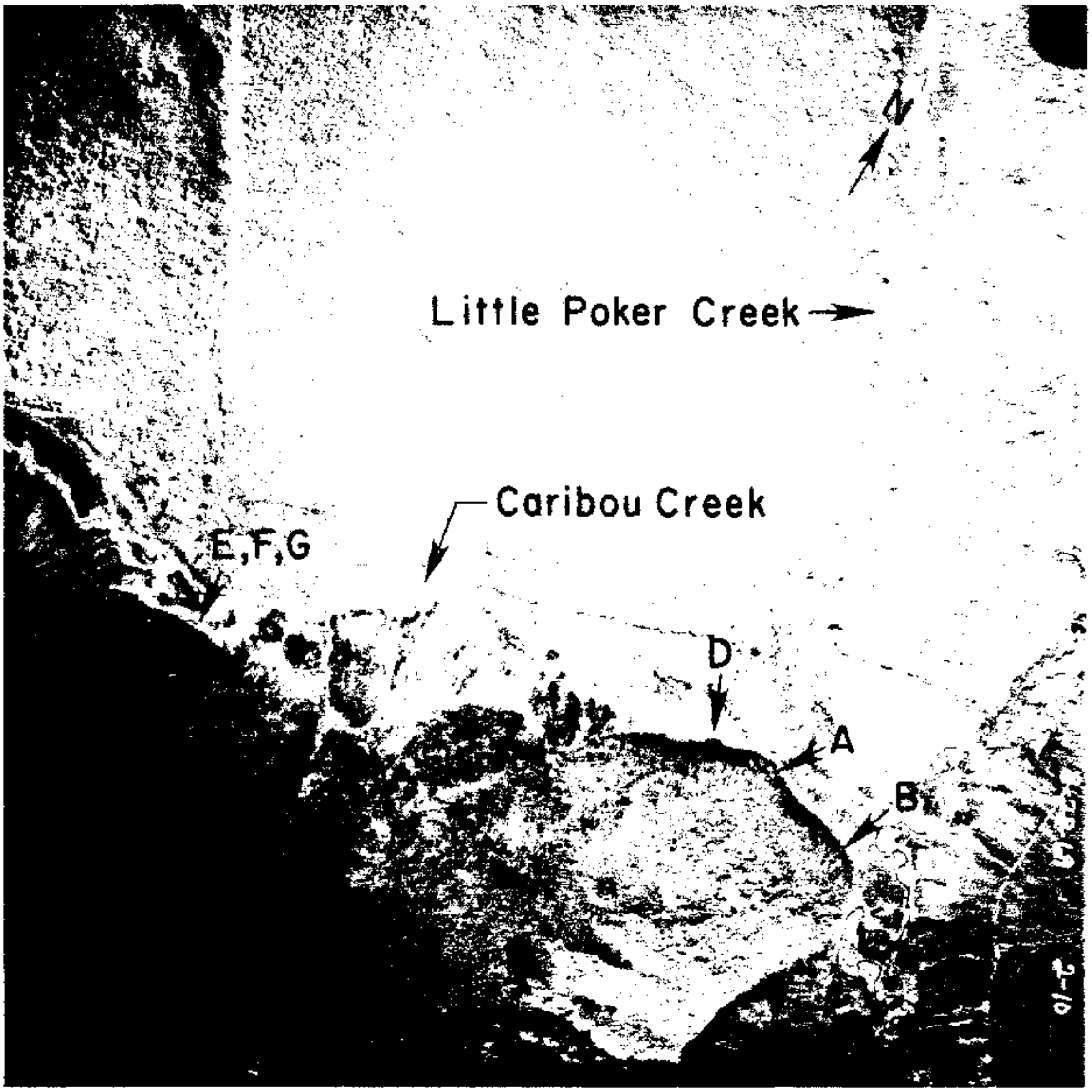

FIG. 1. Air photograph of Caribou and Little Poker Creek Watershed. D, E, F, and G indicate slopes that show signs of movement.

from weathering of the bedrock, was found below the brown silt. Permafrost was encountered at about 50 cm below the surface of the moss, unless bedrock was found at smaller depths.

Figures 3 and 4 show the soil profiles at sections B and F. The profile at section B is quite regular and similar to those at sections A and D. The profile at section F is irregular and is similar to that at E. Note that at FP4 (Fig. 4) moss was found below a layer of silt. This suggests that the soil had overridden the lower moss during an earlier slide. Excavation into the steep face of a step revealed the profile shown in Fig. 5. The presence of brown silt with roots below the gray–brown silt and rock fragments also suggests that the lower profile was overridden by a slide. The cross section of a bent tree is shown in Fig. 6. The dark annual rings of compression wood indicate that the tree had been bent for the last 80 years. These observations indicate that localized slope movements have occurred intermittently over the past 80 years or more.

Field measurements

The field measurement program was designed with an emphasis on simple devices that can cover a fairly large

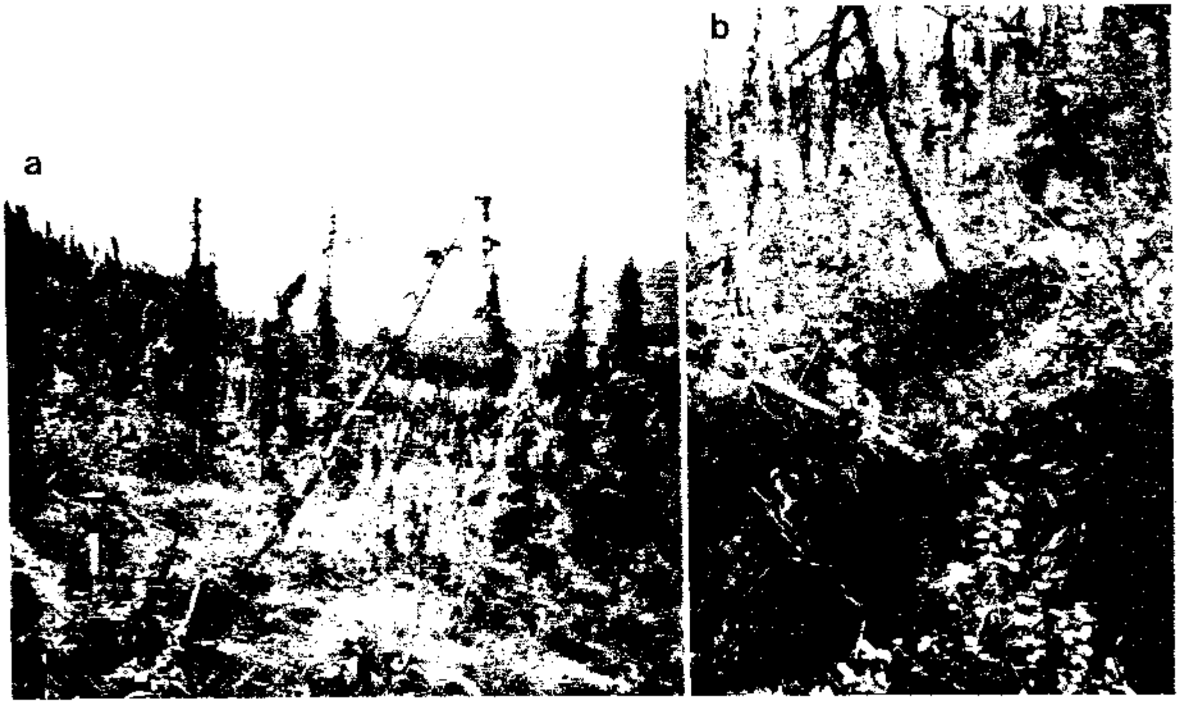

FIG. 2. A slope in Caribou Creek Valley: (*a*) evergreen low savana: black spruce/sphagnum and leaning trees, (*b*) closeup view of a step. The steep face is in the foreground.

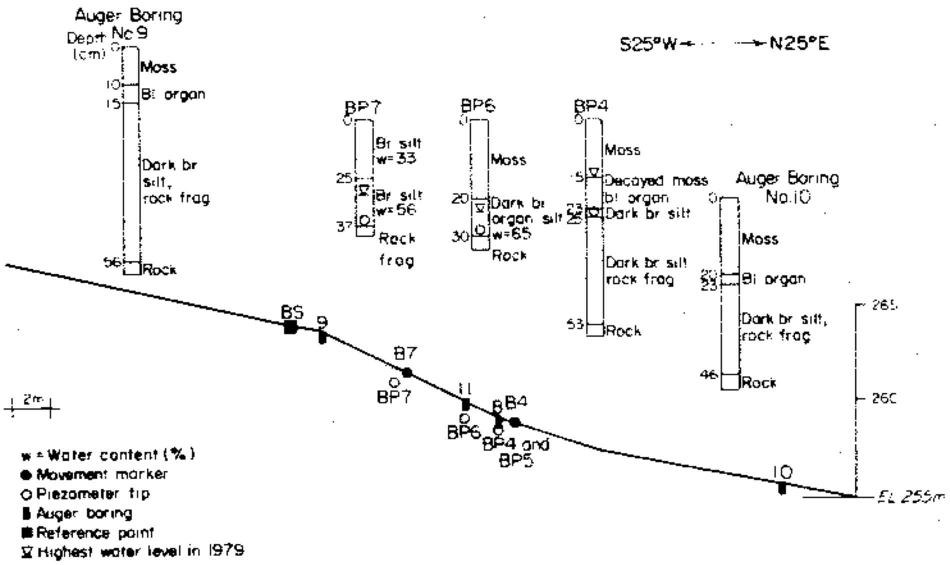

FIG. 3. Soil profile, section B. Symbols BP4 … above soil profiles indicate that the profiles were obtained from auger holes drilled for piezometer BP4 …

area and a variety of observed surface features, and that require little maintenance over a period of several years. Movement markers were set up in rows in the direction of the slope. Each one of the sections had one row of markers, identified by the section symbol (A, B, D, E, F). A sixth row, G, was set in a direction perpendicular to that of E and F. The markers consisted of wooden stakes driven into the moss, where the moss was dense and able to hold the stakes firmly. Otherwise, a wooden rod fastened to a plywood base was used. The base was buried near the bottom of the moss layer. The location of the markers at sections B and F are shown in Figs. 3 and

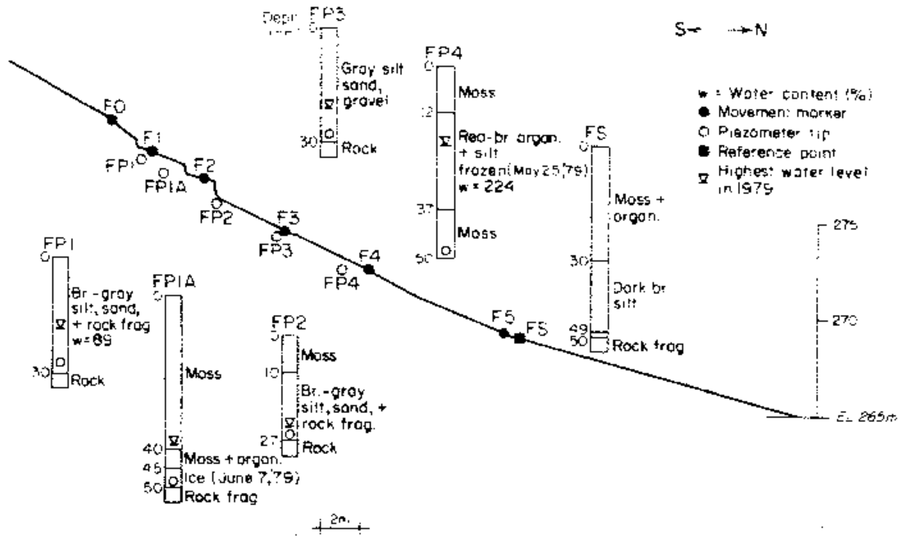

FIG. 4. Soil profile, section F. Symbols FP1 … above soil profiles indicate that the profiles were obtained from auger holes drilled for piezometer FP1 …

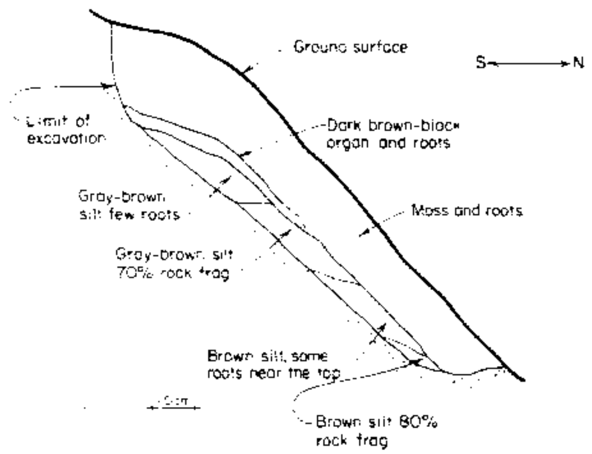

FIG. 5. Soil profile in an excavated step.

4. Plastic tubes with the lower end anchored in rock or permafrost were installed to serve as reference points. These are shown as BS and FS in Figs. 3 and 4. The inclinations of these tubes were checked periodically with a slope indicator. The distances between markers, and between markers and reference points, were measured by tape. Two bench marks were established on bedrock at higher elevations. Theodolite surveys were made in 1981 and 1982 to check the positions of the reference points and selected markers.

Polyvinyl chloride tubes filled with water and fluorescein were buried in the ground and served to indicate the depth of thaw. The piezometers consisted of PVC tubing with a porous filter. In general, piezometer tips were located at the bottom of the brown silt layer and just above the layer of broken rock and gray silt, as shown in Figs. 3 and 4 by the open circles.

FIG. 6. Cross section of a bent tree.

The results of the measurements show that the largest movements occurred at sections E and F. At section D, only two markers had movements of 5 cm during the thawing season of 1979. The movements of the other markers at section D and those at sections A and B were less than 1 cm. Figure 7*a* shows the measured move-

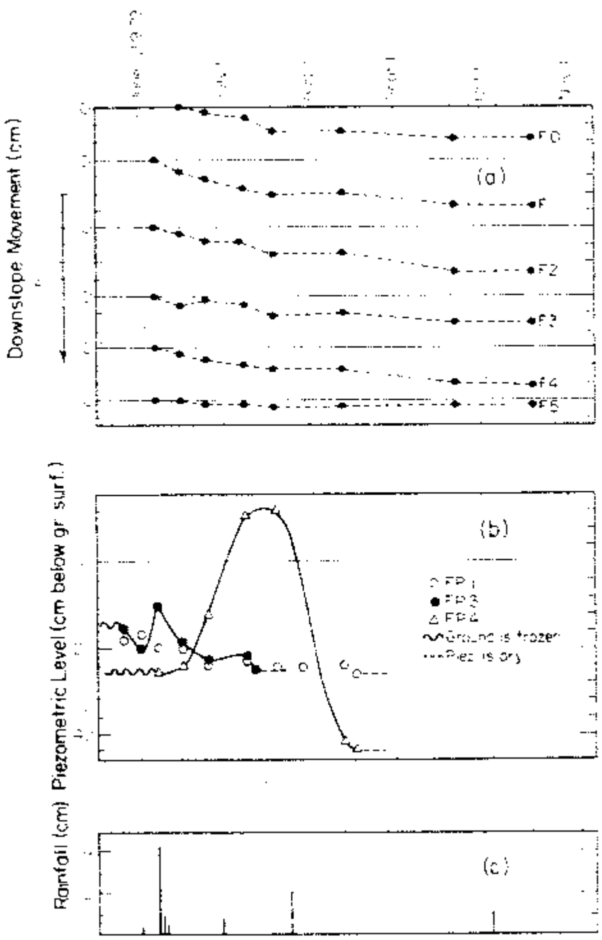

FIG. 7. (*a*) Measured movements, (*b*) measured water levels, and (*c*) rainfall record, summer 1979.

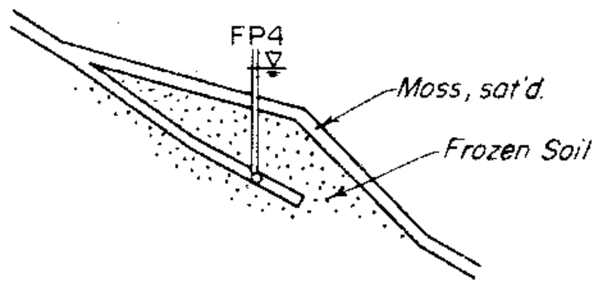

FIG. 8. Hypothetical cross section with a buried moss layer.

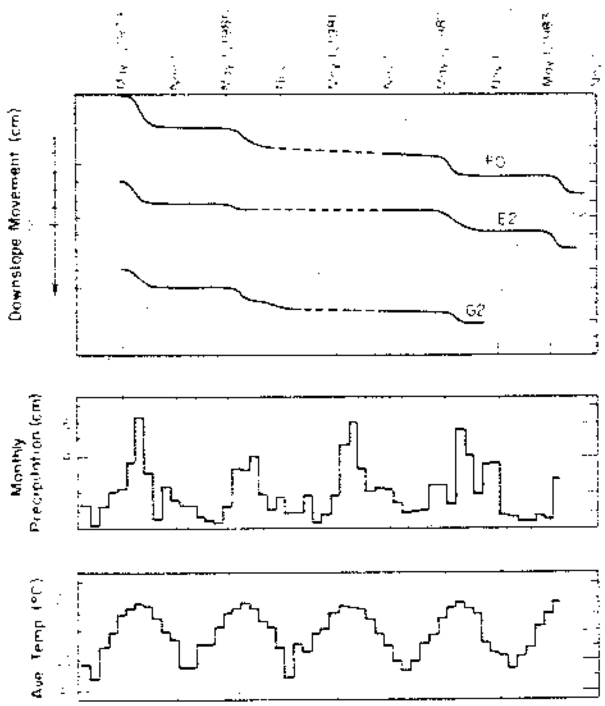

FIG. 9. Marker movements, 1979 to 1983.

ments at section F during the summer of 1979. Examples of observed piezometric levels are shown in Fig. 7*b*. All of the movements took place in June and July.

In most piezometers, the water level rose slightly after the thaw front reached the piezometer tip, as shown for FP1 and FP3. The level then gradually dropped below the level of the piezometer tip. In a few piezometers, the water level rose significantly after thaw. Piezometer FP4 is an extreme case in which the water level rose above the ground surface. On the profile (Fig. 4) we see that FP4 was installed at a depth of 50 cm in a buried moss layer. This suggests that the water in the buried moss layer was connected with the groundwater in the surface moss layer on the uphill side but was surrounded by frozen soil on the downhill side as shown in Fig. 8. Then water would be trapped in the moss layer by the frozen silt around it. As soon as the surrounding soil thawed, the water drained out and the pore pressure dropped rapidly. Examples of measured movements from 1979 to 1983 are shown in Fig. 9 and show the same general pattern as those for 1979.

Soil properties

For general information, water contents were determined for selected samples of organic material and silt. These are shown on the profiles, Figs. 3 and 4. Standard laboratory tests were performed on samples of the soil to determine their particle size distribution and shear strength. The soil is composed of particles of silt size mixed with various proportions of angular rock fragments. Figure 10 shows the range in gradation. Drained direct shear tests were performed on samples of the brown silt obtained by removing all rock fragments larger than 1 mm. The samples were reconsolidated in the laboratory. From the results, an angle of internal friction $\phi' = 30°$ and a cohesion $c' = 0$ were obtained. This is considered to be the lowest possible value of ϕ' for the soil and would apply to a slip surface that passes entirely through the silt. To evaluate the effect of rock

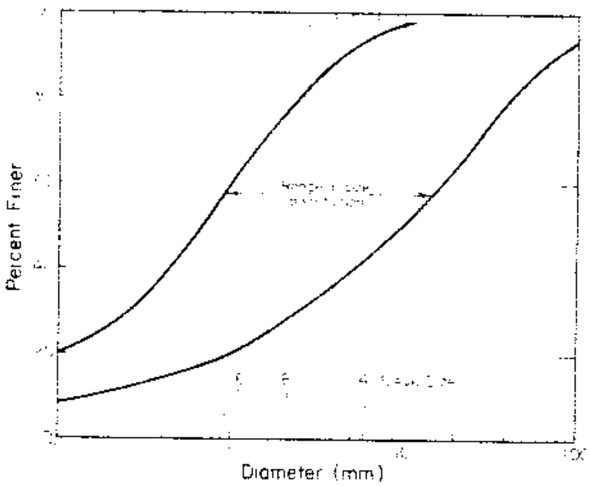

FIG. 10. Particle size distribution of brown silt and gravel.

fragments, samples with rock fragments up to 6 mm were subjected to direct shear tests and a ϕ' of 40° was obtained. Samples containing larger rock fragments could not be tested in the direct shear apparatus. It is known that a well-graded sand has a larger ϕ than a poorly graded sand. It is also known that an angular sand has a larger ϕ than a rounded sand (e.g. Lambe and Whitman 1969). Figure 10 shows that rock fragments greater than 6 mm may constitute up to 50% of the weight of some samples. Hence, these samples should have ϕ' greater than 40°. The conclusion is that $\phi' = 40°$ is a reasonable estimate for the average condition and $\phi' = 30°$ is the lower limit of the shear strength.

Properties of roots and moss

The slopes are covered with a layer of sphagnum moss. The largest trees on these slopes are black spruce. Small trees and shrubs include alder (*Alnus crispa*), dwarf birch (*Betula nana*), bog blueberry (*Vaccinium uliginosum L.*), and Labrador tea (*Ledum decumbens*). The vegetation may influence stability in several ways. Roots that grow downwards serve to tie the moss to the soil, and also tie the soil to the weathered rock. The moss layer and roots that grow parallel to the slope may serve as a tensile reinforcement. If a portion of the slope begins to move, it would be tied by the reinforcement to the stable portion located uphill. To investigate the contribution of the vegetation, excavations were made to study the roots, and tension tests were performed to measure the strengths of the roots and moss.

Results of excavations show that most of the roots are located in the moss and the organic silt. Figure 11 illustrates the roots that grow parallel to the ground surface in the moss and organic silt. Only a small number of roots grows downward into the different soil layers. Very few enter the zone of broken rock.

The tensile strength of roots was measured. Samples of root were clamped in the grips of a testing machine and loaded to failure. The results are plotted in Figure 12. The data fall well below those reported by Wu *et al.* (1979) and those summarized by Gray (1978).

To evaluate the tensile strength of the moss, blocks of the sphagnum moss were excavated and subjected to the tension test. The tensile strength varied over a wide range depending upon the number and size of woody roots that were present in the moss. Several representative stress–strain curves are shown in Fig. 13. Sample No. 1 contained no woody roots while samples 2a, 2b, and 3 contained various amounts of woody roots.

To evaluate the contribution of the woody roots to the moss strength, the moss samples were torn apart after the test and roots larger than 1 mm in diameter were counted. Figure 14 shows the roots found in sample 3. At the end of the test (strain = 0.60) the right half of the sample was still held together by these roots, while the moss in the left half had already separated (Figs. 14 and 15). The strength of the right half was estimated by adding the tensile strengths of the intact roots shown in Fig. 14 to the tensile strength of the intact moss. The strength of the moss was taken to be 2.5 kPa. This gave a strength of 3.8 kPa and is shown as a triangular point at a strain of 0.6 in Fig. 13. The maximum possible strength of the block was estimated by adding the tensile strengths of all roots shown in Fig. 14 to the tensile strength of the entire cross section of the moss. This gave a strength of 6.7 kPa. This is shown as a triangular point at a strain of 0.37 in order to compare it with the measured peak strength. The measured stress–strain curve falls below these points. This is expected because not all of the woody roots would be loaded to their tensile strength at the same time. Results of similar calculations for the other samples are also shown in Fig. 13. The conclusion is that the use of the full tensile strength of the woody roots leads to an overestimate of the strength of the moss layer by 0–1.5 kPa, or 0–50%.

The strength of the root–moss complex may also be estimated for the roots shown in Fig. 11. The strength of the moss is 2.5 kPa and the average thickness of the moss layer is approximately 20 cm. To this should be added the contribution of the root system. For a given cross section, not all the roots that intersect this section will be loaded to their tensile strengths simultaneously. It is reasonable to expect that the roots aligned in the direction of the tensile force will receive the largest load and will fail first. To estimate the contribution of the roots in Fig. 11, it was assumed that only those roots that run in the direction of the slope ±30° would fail in tension. The tensile strengths of these roots were added to the moss strength to obtain the strength of the root–moss complex. The computed tensile strength of the root–moss complex lies between 3.5 and 7.0 kPa,

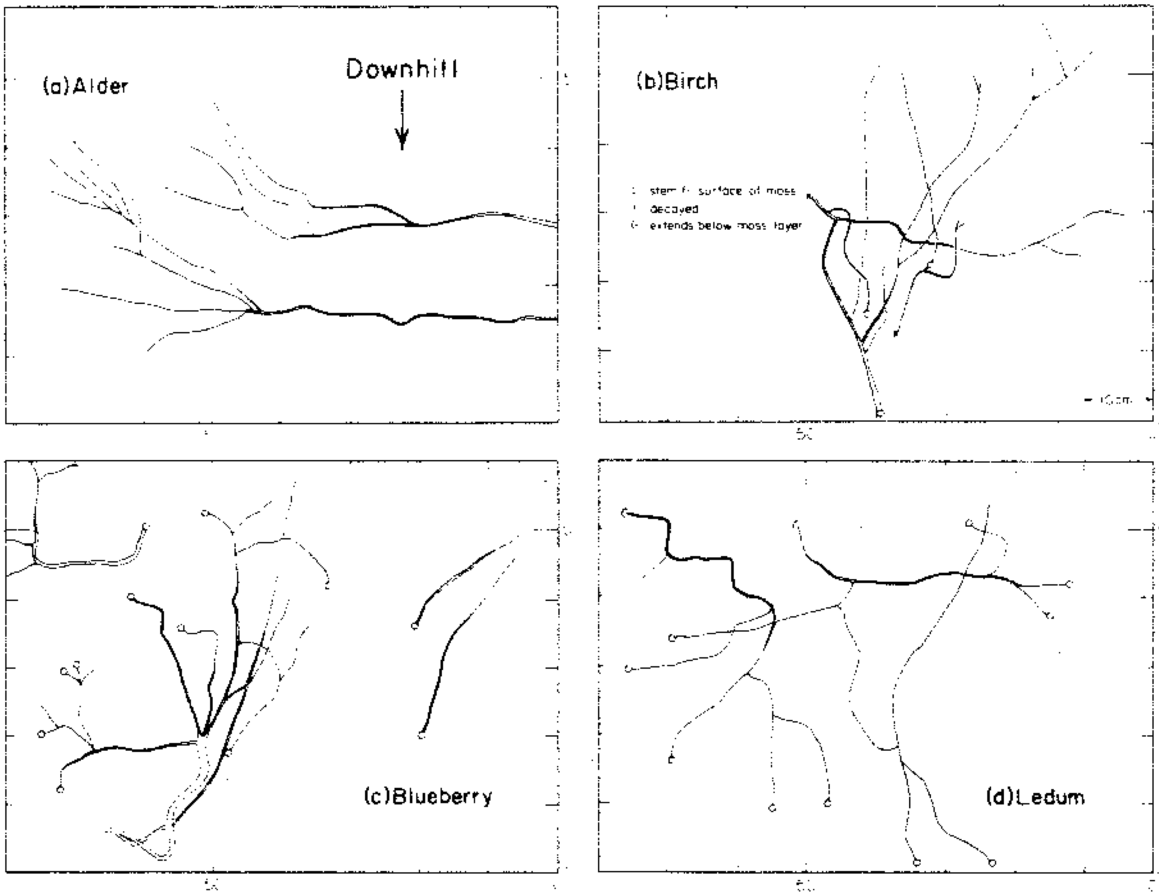

FIG. 11. Excavated roots of (*a*) alder, (*b*) birch, (*c*) blueberry, and (*d*) ledum in an area 60 cm × 80 cm.

depending on the cross section chosen. This is approximately the same as the range in measured strength shown in Fig. 13. These limited data indicate that the average strength of the moss–root complex is of the order of 5 kPa.

Stability analysis

Two types of stability analyses were performed. In the first, an infinite slope was assumed. This would be applicable to sections B and D, where the soil profile is relatively uniform. The idealized section is shown in Fig. 16. The critical slip surface is considered to be at the boundary between the brown silt and the gray silt. Because the gray silt contains a high percentage of gravel and rock fragments, its strength should be much higher than that of the brown silt. Since very few roots penetrate into the gray silt and rock, the contribution of root strength to the shearing resistance may be ignored. The water level is taken to be at the surface of the silt. The values of α, h_1 and h_2 are listed in Table 1. The values of $c' = 0$, $\phi' = 40°$ are considered to be reasonable averages for the shear strength of the silt. The computed safety factors (Table 1) are close to 1 for both sections. The minimum shear strength of the silt is $c' = 0$, $\phi' = 30°$. The computed safety factors are less than 1 for both sections. The value of $\phi' = 30°$ is most likely too low because of the presence of rock fragments.

The application of the infinite slope analysis to sections E and F involves more uncertainties because of the variability in the soil profile and the pore presure. If it is assumed that the soil profile, prior to the disturbance, is the same as that shown in Fig. 16, then the computed safety factors are well below 1 (Table 1). Thus, according to the results of the infinite slope analysis, sections E and F should have failed and sections B and D are barely stable.

One important feature is that the rate of thaw is not uniform over the entire slope. Some areas thaw before others. In this case, the entire slope cannot fail as assumed in the infinite slope analysis. To analyze the case of a localized thaw, consider a wedge of thawed soil abc (Fig. 17). The depth h_2 is the thickness of the brown silt. The dimension a is arbitrarily chosen to be equal to the average size of a step, because the hypothesis is that if the wedge fails, it will be displaced to form a step. The

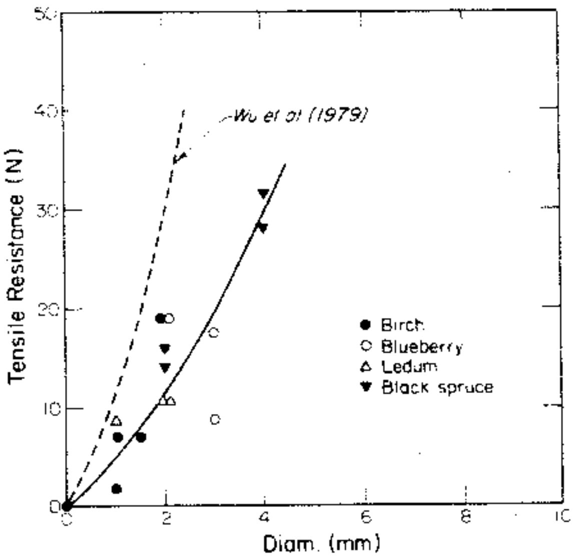

FIG. 12. Tensile strength of roots.

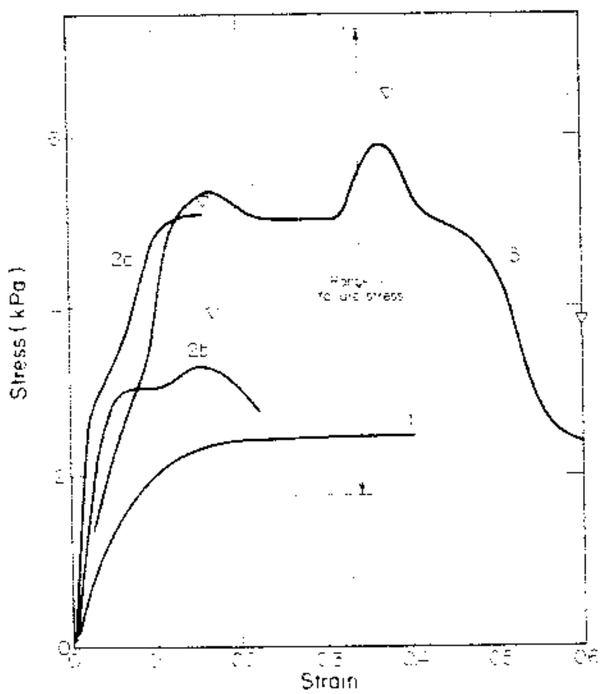

FIG. 13. Stress–strain curves of moss.

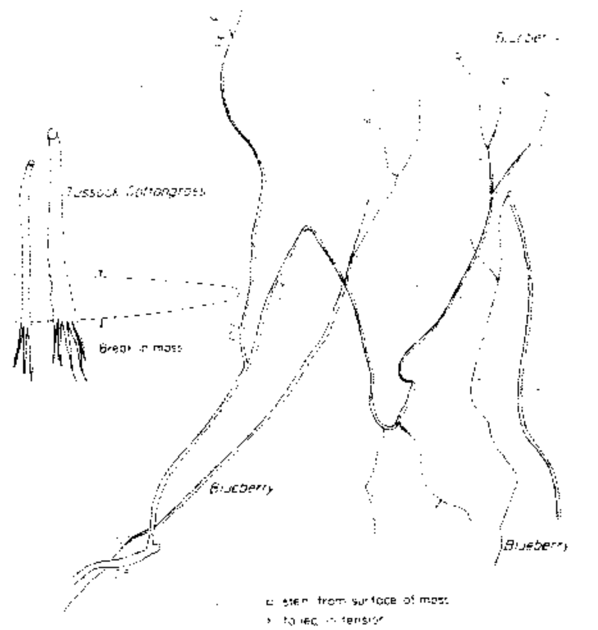

FIG. 14. Roots in moss sample No. 3: numbers indicate root diameter in cm.

FIG. 15. Tension test, moss sample No. 3.

water level is assumed to be at the surface of the silt, as before. Immediately upon thaw the drainage will be toward the free surface. For simplicity, it is assumed that seepage is parallel to the slope and the error is small. Then, the resultant pore pressure on the potential failure surface is

$$[1] \quad U = \frac{1}{2}\gamma_w h_2 l \cos^2 \alpha$$

and the weight of the wedge is

$$[2] \quad W = \frac{1}{2}\gamma a h_2$$

where γ_w, γ = unit weight of soil and water, respectively.

The safety factor against a shear failure on ab is

TABLE 1. Computed safety factors

				Safety factor for:					
				Infinite slope		Wedge		Step	
Section	α (deg)	h_1 (cm)	h_2 (cm)	φ′ = 30°	φ′ = 40°	φ′ = 30°	φ′ = 40°	φ′ = 30°	φ′ = 40°
B	21	20	20	0.72	1.05	1.50	1.88	—	—
D	25	20	20	0.66	0.95	1.18	1.45	—	—
E	30	20	20	0.50	0.70	0.84	1.03	(a) 0.91 (b) 0.90	(a) 1.24 (b) 1.21
F	30	20	20	0.50	0.70	0.84	1.03	(a) 0.91 (b) 0.90	(a) 1.24 (b) 1.21

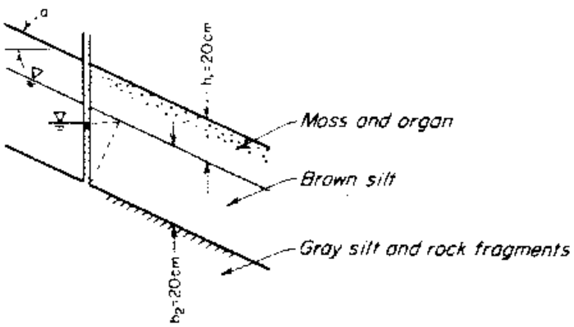

FIG. 16. Stability analysis of infinite slope.

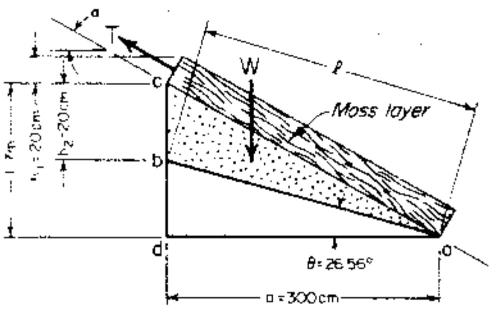

FIG. 17. Stability analysis of a thawed wedge.

$$[3] \quad F_S = \{[W\cos\theta - U - T\sin(\alpha-\theta)]\tan\phi' + T\cos(\alpha-\theta)\}/W\sin\theta$$

where T = tension in the moss layer. If the average strength of the moss–root complex is taken to be 5 kPa, the value of T is 1 kN/m. The calculated values of F_S are also shown in Table 1. They are well above 1 for sections B and D and close to 1 for E and F. Thus, if thaw is limited to areas 3 m × 3 m, failure is unlikely on sections B and D, but likely on sections E and F.

If failure of the thawed wedge occurs, the wedge moves downslope and one may hypothesize that a step is formed as shown in Fig. 18. The third stability analysis considers the stability of a step. The problem is simplified by using a two-dimensional analysis as shown in Fig. 19. This ignores the resistance offered by the moss on the sides (abc in Fig. 18). The measured water

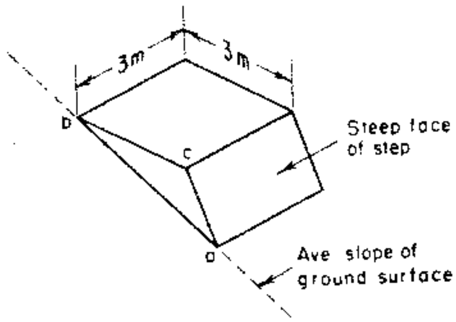

FIG. 18. Simplified sketch of a step.

level in a step varies between 0 and 20 cm below the top of the silt (FP1, FP1A, and FP3), and an average of 10 cm is assumed. Figure 19 shows two assumptions for the water level: (a), where the water surface is parallel to the flat surface of the step and (b), where the height of the water level above ab is proportional to the height of the thawed silt. The seepage is again assumed to be parallel to the failure surface ab for both cases. For (a)

$$[4] \quad U = \frac{1}{2}\gamma_w h_w l_w \cos^2\alpha$$

and for (b)

$$[5] \quad U = \frac{1}{2}\gamma_w h_w l \cos^2\alpha$$

For both (a) and (b)

$$[6] \quad W = \frac{1}{2}\gamma a(a-h)(\tan\alpha - \tan\theta)$$

and

$$[7] \quad F_S = \frac{(W\cos\alpha - U)\tan\phi' + T}{W\sin\alpha}$$

The computed values of F_S for φ′ = 30° and 40° are given in Table 1. They are somewhat larger than the values for a wedge. Thus, if a wedge fails and develops into a step, the latter may become stable.

All of the values of F_S shown in Table 1 were computed for conditions considered to represent the

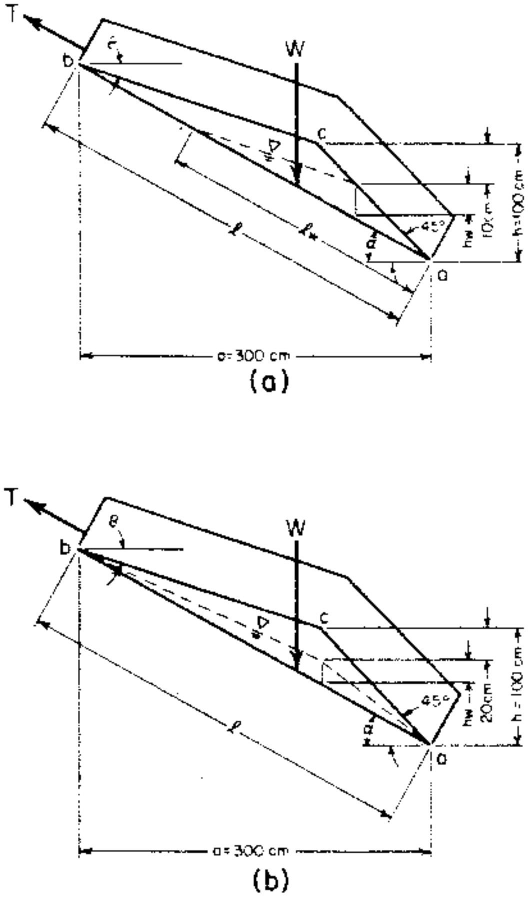

FIG. 19. Stability analysis of a thawed step.

average. Because of the spatial variations in geometry, soil and vegetation properties, and spatial and temporal variations in pore pressure, the departure from the average may be substantial and where conditions are unfavorable, local failures may occur. The occurrence of these local failures is supported by the presence of breaks in the moss layer near F1 and the relative movement of F1 with respect to F0 and F2 (Fig. 7).

At this point, it is worthwhile to consider the observed slope behavior in the light of other studies of slope creep in cold regions. There have been many studies of solifluction and gelifluction, and different mechanisms have been suggested (e.g., Harris 1977; McRoberts and Morgenstern 1974; Washburn 1967, 1980; Williams 1957, 1966). Both Harris and McRoberts and Morgenstern related the movements to shear failure under high pore pressures during thaw. Harris attributed the high pore pressure at Okstinden to saturation of the thawed soil by infiltration of meltwater. McRoberts and Morgenstern have shown that excess pore pressures may develop during thaw if the thaw–consolidation ratio R is large, and that this can be a cause of slope instability on flat slopes. The results of the present study are in agreement with the observations of Harris and of McRoberts and Morgenstern in that the movements are attributed to instability when the shear strength is reduced by high pore pressures. In the present study, most of the pore pressures measured immediately after thaw are close to or less than hydrostatic. Rough calculations with the thaw–consolidation theory (Morgenstern and Nixon 1971) have shown that the excess pore pressure should be small. Observed excess pore pressures are believed to be the result of localized conditions.

Summary and conclusions

Ground movements and pore pressures were measured on several north-facing hillside slopes along Caribou Creek near Fairbanks. Movements in the downhill direction were observed on slopes whose inclinations are close to 30°. These movements occurred almost entirely during early summer. At that time the piezometric levels were also at their highest. Thawing of the ground progressed nonuniformly. The water level in a piezometer generally rose a few centimetres after the thaw front reached the piezometer tip and then dropped gradually.

Excavations were made to measure the numbers and dimensions of woody roots present in the soil and tests were made to measure the tensile strength of the moss and of the moss–root complex.

Stability analyses made for an infinite slope show that the safety factors are 1 or lower. However, thaw does not occur uniformly over an entire slope and the pore pressures do not reach the maximum at the same time. Hence, failure of the entire slope is unlikely. If thaw occurs first over a limited area of 3 m × 3 m, a wedge of the thawed material may move downhill. Stability analysis of such a wedge shows that the safety factor is close to 1 on slopes with an inclination of 30°. Hence, such slides are possible. The hypothesis is that when a wedge slide took place the soil was displaced to form a step. Stability analyses for a step show that safety factors are slightly larger than 1. Thus the step could remain stable after a wedge slide had occurred. Stability analysis of the wedge and step took into account the tensile strengths of the moss layer and of the roots. The strength of the moss–root complex was found to contribute significantly to the stability of the wedge and of the step.

Acknowledgments

The work reported in this paper was supported by the Pacific Northwest Forest and Range Experiment Station, U.S. Forest Service (Grants 37-PNW-77 and 52-PNW-78), and by the National Science Foundation (Grant CEE-8113253). Logistics for fieldwork were provided by the Institute of Northern Forestry, Fairbanks, AK. The writer wishes to thank the personnel of the Institute for their generous help. C. W. Slaughter, A. E. Helmers, and J. E. Lynch participated in the planning and the execution of the field measurements. Their contributions are gratefully acknowledged.

GRAY, D. H. 1978. Role of woody vegetation in reinforcing soils and stabilizing slopes. Symposium on Soil Reinforcing and Stabilizing Techniques, Sydney, pp. 253–306.

HARRIS, C. 1977. Engineering properties, groundwater conditions, and the nature of soil movement on a solifluction slope in North Norway. Quarterly Journal of Engineering Geology, **10**, pp. 27–43.

LAMBE, T. W., and WHITMAN, R. V. 1969. Soil mechanics. John Wiley & Sons, New York, NY.

MCROBERTS, E. C., and MORGENSTERN, N. R. 1974. The stability of thawing slopes. Canadian Geotechnical Journal, **11**, pp. 447–469.

MORGENSTERN, N. R., and NIXON, J. F. 1971. One-dimensional consolidation of thawing soils. Canadian Geotechnical Journal, **8**, pp. 558–565.

RIEGER, S., FURBUSH, C. E., SHOEPHORSTER, D. B., SUMMERFIELD, H., JR., and GEIGER, L. C. 1972. Soils of the Caribou–Poker Creeks Research Watershed, Interior Alaska. Technical Report 236, U.S. Army, Cold Regions Research and Engineering Laboratory, Hanover, NH. 11 p.

SLAUGHTER, C. W. 1971. Caribou–Poker Creek Research Watershed, Interior Alaska. Special Report 157, U.S. Army, Cold Regions Research and Engineering Laboratory, Hanover, NH.

VIERECK, L. A. 1975. Forest ecology of the Alaska taiga. Proceedings Circumpolar Conference on Northern Ecology, Ottawa, I-1-22.

WARHAFTIG, C. 1965. Physiographic divisions of Alaska. United States, Geological Survey, Professional Papers, No. 482, 52 p.

WASHBURN, A. L. 1967. Instrumental observations of mass-wasting in the Mesters Vig District, Northeast Greenland. Meddelelser om Groenland, **166**(4), 318 p.

——— 1980. Geocryology. John Wiley & Sons, New York, NY. 406 p.

WILLIAMS, P. J. 1957. Some investigations into solifluction features in Norway. Geographic Journal, **123**, pp. 42–58.

——— 1966. Downslope soil movement at a subarctic location with regard to variations with depth. Canadian Geotechnical Journal, **3**, pp. 191–203.

WU, T. H., MCKINNELL, W. P., III, and SWANSTON, D. N. 1979. Strength of tree roots and landslides on Prince of Wales Island, Alaska. Canadian Geotechnical Journal, **16**, pp. 19–33.